



Project no. TIP5-CT-2006-031415

INNOTRACK

Integrated Project (IP)

Thematic Priority 6: Sustainable Development, Global Change and Ecosystems

D4.2.1

The impact of vertical train-track interaction on rail and joint degradation

Due date of deliverable: 2007-08-31

Actual submission date: 2007-11-15

Start date of project: 1 September 2006

Duration: 36 months

Organisation name of lead contractor for this deliverable:

Chalmers

Revision: Final 1

Project co-funded by the European Commission within the Sixth Framework Programme (2002-2006)		
Dissemination Level		
PU	Public	√
PP	Restricted to other programme participants (including the Commission Services)	
RE	Restricted to a group specified by the consortium (including the Commission Services)	
CO	Confidential, only for members of the consortium (including the Commission Services)	

Table of Contents

Glossary	2
1. Executive Summary	3
2. Introduction	4
3. Collection of input and validation data	5
3.1 Measurements of axle loads on selected lines.....	5
3.2 Data on rail/joint degradation.....	6
3.3 Rail material data.....	6
3.4 Squat monitoring.....	6
4. Numerical simulations of high-frequency train-track dynamics and subsequent deterioration	8
4.1 Background – Numerical models.....	8
4.2 Influence of corrugation and out-of-round wheels	9
4.3 Growth of large rail cracks.....	11
4.4 Influence of insulated joints	11
5. Numerical simulations of squats	12
5.1 Correlation analyses	12
5.2 Numerical models.....	12
5.3 Influence of rail top irregularities and material strength.....	13
5.4 Influence of traction/braking and unsprung mass.....	13
5.5 Influence of welds of continuously welded rails.....	13
5.6 A squats growth process is postulated	14
6. The effect of material characteristics on material deterioration	18
7. Conclusions	19
8. Annexes.....	20

Glossary

DIFF	Dynamisk Interaktion Fordon–Farbana (Dynamic interaction train–track); in-house code for simulations of dynamic train–track interaction
FIERCE	Fatigue Index Evaluator for Rolling Contact Environments; in-house code for evaluation of rolling contact fatigue impact
FE	Finite element
OOR	Out-of-roundness
RCF	Rolling contact fatigue
SP	Sub Project
WP	Work Package

1. Executive Summary

In this tentative report we present a summary of the work carried out during approximately the first nine months of the INNOTRACK project regarding the influence of rail/joint degradation on operational loads and subsequent deterioration. The focus is here on the vertical train-track interaction and related deterioration.

The work within this field can be divided in two categories. The first concerns the collection of input and validation data. In this category the current deliverable includes measurements of in-field axle loads, in-field monitoring of squats and compilation of material data.

The second category is the actual numerical simulation and resulting quantifications of increased operational loads and deteriorations. Here the deliverable includes a state-of-the-art study of the effect of material characteristics on material deterioration and the practical implications. Further, the deliverable contains reports of parametric studies of the influence of rail corrugation, the growth of larger rail cracks, the influence of the design of insulated joints and the influence of rail squats.

2. Introduction

The overall objectives of Work Package (WP) 4.2 are (see the INNOTRACK Description of Work):

- To evaluate tolerances and limits for rails and joint degradation in terms of allowable magnitudes of wear, corrugation, geometrical deviations, etc under different operational conditions.
- To establish minimum action rules for the occurrence of material defects under different operational conditions and rail/joint degradation

This deliverable is the first step towards the first objective.

To further detail the contributions of WP 4.2 and its interaction to other Sub-Projects (SP) and WPs, it was clarified at the WP 4.2 meeting 15th of February 2007 that the focus in WP4.2 is mainly on vertical train-track interaction and related. In addition longitudinal forces due to braking/traction will be included when suitable. Analysis of lateral train-track interaction and subsequent deterioration calls for vehicle models that are largely lacking or are not available for use in INNOTRACK. This topic is therefore left for the low- and medium-resolution modelling of SP1. This includes e.g. prediction of the formation of head checks. In addition to SP1, lateral train-track dynamics and subsequent deterioration will also to some extent be studied in SP3 and WP4.3.

Within these frames, the work within WP4.2 includes the collection of input and validation data and actual numerical simulation and resulting quantifications of increased operational loads and deteriorations.

3. Collection of input and validation data

To support numeric simulations, a multitude of input data is needed. This includes background information that will allow for simulation of train track dynamics and subsequent material deterioration, as well as in-field data to validate results from numerical simulations.

3.1 Measurements of axle loads on selected lines

Banverket is carrying out a measuring campaign, where the traffic on selected lines is classified in detail. So far information of annual loads has been collected for line 119 (Luleå – Boden) and line 611 (Falköping – Alingsås). For line 119 the annual load estimation is based on measurements from wheel impact load detectors. For line 611 the loads are mainly estimated of train weights given by the train operators. Data for line 119 have been confirmed by measurements. In-depth measurement for line 611 will start in June 2007.

Results from the measuring campaign so far are displayed in Figure 1 and Figure 2. The graphs are based on number of axles passed a hot wheel detector for different type of trains and an assumption on the axle weight distribution (mean and standard deviation) for each train type.

For the other two lines intended to be included in the study (line 910 and 111) the work has not yet started. The loads on line 910 will be estimated, whereas for line 111 there are measurements of a wheel impact load detector that can be used.

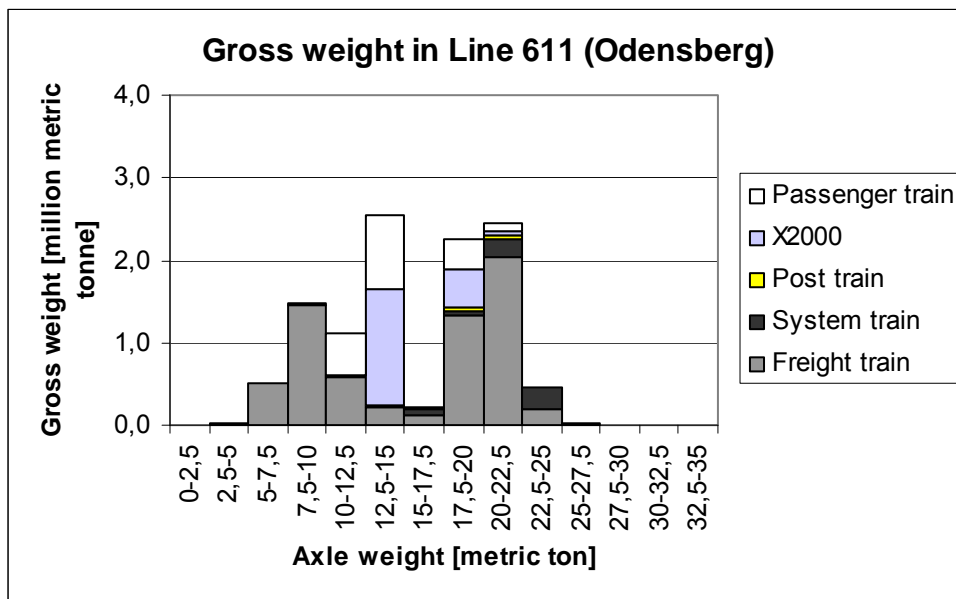


Figure 1 Gross tonnes per year for train passing the detector in Odensberg (line 611)

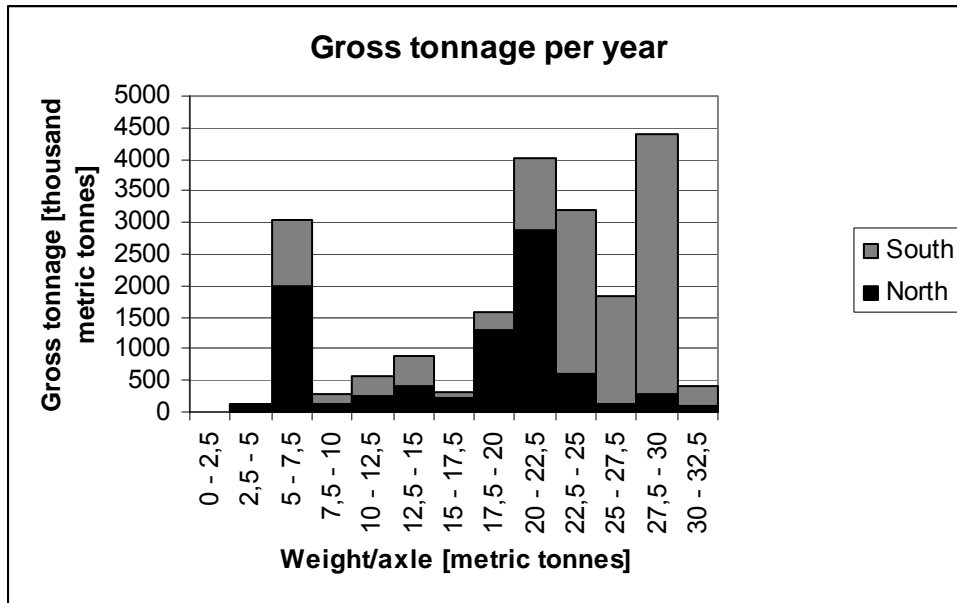


Figure 2 Gross tonnes per year for train passing the detector in Sunderbyn (line 119)

3.2 Data on rail/joint degradation

Banverket will provide field observations and measurement results. So far no direct data collection has been made. There are however measurements the track recording car (STRIX) that can be used to see the trends on specific places. Banverket are awaiting results from Corus rail to choose such places.

3.3 Rail material data

The study of rail deterioration to be carried out within INNOTRACK relies on available material data of the rail steels to be studied. These data are essential for the numerical simulations of material deterioration that are a core part in the search for innovative solutions. To this end, voestalpine has collected data on their current steel grades. These data are compiled in Appendix I.

3.4 Squat monitoring

Squat monitoring has been planned by ProRail and TU Delft to provide data for WP4.2. Five monitoring locations were selected in November 2006. But due to the aggressive corrective and preventive grinding program carried out on the ProRail network, 4 of the 5 selected track sections have been ground. Selection of 4 new sections is actively underway. The intention is still to monitor a total of 15 squats in 5 track sections. In the mean time, 2 new locations have been selected. The first round of measurement on the currently selected 3 locations has been carried out. The intention is to monitor a total of 15 squats.

It has to be emphasized that due to grinding planning and safety considerations, the final remaining monitored locations may be reduced to 1 or 2, after an intended period of 2 years, though great care will be taken to save the squats from being removed.

The intended measurements include:

- Longitudinal rail top geometry
- Lateral rail top geometry
- Local track dynamic characteristics

The following major considerations have been / will be taken into account for the selection of locations and squats:

- Varieties of locations
- Focus on concrete sleeper
- Most are of class A and B (according to ProRail visual inspection criteria)
- Some squat C. They should not be severe, especially without crack, or with only shallow cracks, so that they are considered not dangerous in the coming 2 years
- When selecting class A squats, most of them should have wave pattern after/following them
- Some at wooden sleepers
- Some at welds

4. Numerical simulations of high-frequency train-track dynamics and subsequent deterioration

4.1 Background – Numerical models

The computer program DIFF is used to simulate vertical train-track interaction at high frequencies, from about 20 Hz to at least 2000 Hz. A principal sketch of the model is shown in Figure 1. Results from two field test campaigns have been used to validate the train-track interaction model [1]. The first test case involved impact loads from a wheel flat, while the other case studied the influence of a corrugated rail on dynamic vertical contact forces. The track model was calibrated versus test data from laboratory and field tests. Input data on rail and wheel roughness were taken from field measurements. Good agreement between calculated and measured vertical contact forces was observed, both with respect to magnitude and frequency content, for most frequencies below 2000 Hz. The best agreement was obtained when a train model that accounted for both wheelsets in a bogie was used (instead of using a single wheelset model). Based on the good and consistent agreement between measured and simulated vertical contact forces, it is argued that the computer program DIFF is a useful tool in investigations of vertical dynamic train-track interaction at high frequencies. See reference [1] for more details.

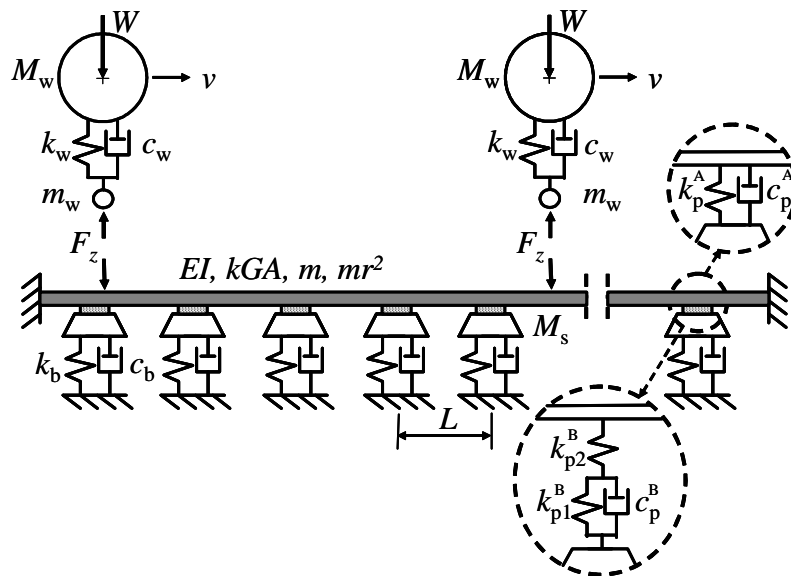


Figure 3 *Principal sketch of dynamic train-track interaction model in DIFF. Train model with two wheelsets and two alternative visco-elastic models of the rail pad are shown. From [1]*

Results from DIFF have been used as input to FIERCE for prediction of rolling contact fatigue (RCF) impact. The influence of short-pitch rail corrugation and wheel out-of-roundness (OOR) on RCF of a high-speed passenger train has been investigated, see [2]. It is shown that the corrugation and the OOR have a profound effect in that levels of wheel and rail irregularities that have been measured in the field may be sufficient to generate subsurface initiated RCF, see examples in Figure 2. In particular, the high-frequency content of the contact forces is of importance. Errors induced by neglecting such high-frequency components in measurements and/or simulations have been investigated by comparing RCF indices based on contact forces that have been low-pass filtered with various cut-off frequencies.

A major benefit with the FIERCE model is that it, in a simple manner, clarifies the relations between the parameters that have an influence on RCF. For example, it can be seen that a poor contact geometry (as defined by small contact semi-axes, a and b) will increase the risk for surface initiated fatigue. However, surface fatigue initiation will only occur if the traction is high enough. If traction is managed in a proper manner, e.g. by lubrication or bogie design, surface fatigue may be avoided even at poor track conditions.

However, the poor contact conditions may in such circumstances instead be reflected by an increase in subsurface fatigue initiation. Under such circumstances, the only way of preventing RCF is to decrease the contact loading or to improve the contact geometry, e.g. by rail grinding and/or wheel re-profiling. To avoid cracking due to RCF, a maximum roughness level in the wavelength interval up to 10 cm is proposed, see [2].

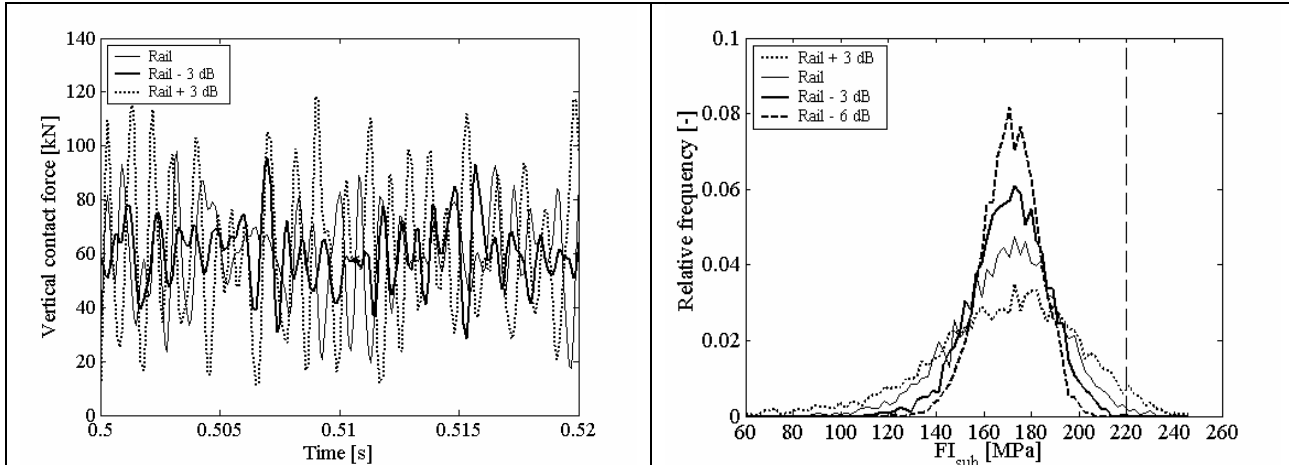


Figure 4 Partition of calculated time history of vertical wheel–rail contact force corresponding to different rail roughness spectra (left) and corresponding relative frequency of subsurface fatigue index FI_{sub} (equal to the maximum Dang Van stress, see e.g. Appendix II) with estimated reduced fatigue limit in shear indicated (right). Trailer wheelset on high-speed train X2000 at $v = 200$ km/h. From [2]

To analyse the consequences of insulated rail joints, DIFF has been combined with analysis of material deterioration in terms of rolling contact fatigue (RCF) and plastic deformations, see [3]. The insulated joints form local rail irregularities and lead to a local change of dynamic track stiffness. These effects lead to high contact load magnitudes. Owing to the negligible load carrying capacity of the insulating material, high stress concentrations and pertinent plastic deformations will occur at the insulated joint. Finally, it was found that the dynamic excitation caused by the rail joint will lead to increased RCF impact also at some distance from the joint.

References

- [1] Jens Nielsen: High-frequency vertical wheel–rail contact forces – validation of a prediction model by field testing, *Proceedings 7th International Conference on Contact Mechanics and Wear of Rail/Wheel Systems (CM2006)*, Brisbane (Australia) September 2006, vol 1, pp 41-48
- [2] Jens Nielsen, Anders Ekberg and Roger Lundén: Influence of short-pitch wheel/rail corrugation on rolling contact fatigue of railway wheels, *IMechE Journal of Rail and Rapid Transit*, vol 219, no F3, 2005, pp 177-187
- [3] Elena Kabo, Jens Nielsen and Anders Ekberg: Prediction of dynamic train/track interaction and subsequent material deterioration in the presence of insulated rail joints, *Vehicle System Dynamics*, vol 44, Supplement, 2006, pp 718–729

4.2 Influence of corrugation and out-of-round wheels

As discussed in section 4.1, the influence of rail corrugation on risks for RCF has been investigated in a previous study that focused on train–track dynamics. A subsequent study has been carried out to focus on RCF mechanisms and parametric influence. As described in section 4.1, the study featured simulations of high-frequency train–track dynamics using DIFF, and fatigue impact evaluation using FIERCE. The study is included in Appendix II.

Some conclusions of the study:

- Corrugation will increase rolling contact fatigue impact by two mechanisms
 - The roughness of the rail surface will cause an increase in contact load magnitudes due to its influence on the dynamic train-track interaction. This is the dominating cause of high fatigue impact in high-speed operations. This effect is partly counter-acted by the increased size of the Hertzian contact patch due to the high load magnitudes.
 - The poor contact geometry owing to the corrugation may also by itself be a cause to an increased fatigue impact. This is mainly a case for very low-speed operations.
- Higher axle loads will increase RCF impact.
- An increase in un-sprung mass will have no effect on fatigue impact providing the static axle load is not affected.
- For the operational conditions studied, corrugation is more of an issue in high-speed operations as compared to heavy haul. This is in line with operational experience.

It should be kept in mind that these conclusions relate to vertical train-track interaction and consequently the initiation and growth of subsurface cracks in rails and wheels. If traction and/or braking is included in the analysis there will be an equal spread in interfacial friction, as shown in Figure 5. This may lead to the formation of surface initiated fatigue.

Figure 5 also shows the influence of the high-frequency content of the loading when analysing the influence of corrugation (through simulations or measurements). As seen, low-pass filtering with a cut-off frequency of 90 Hz results in almost quasi-static predictions.

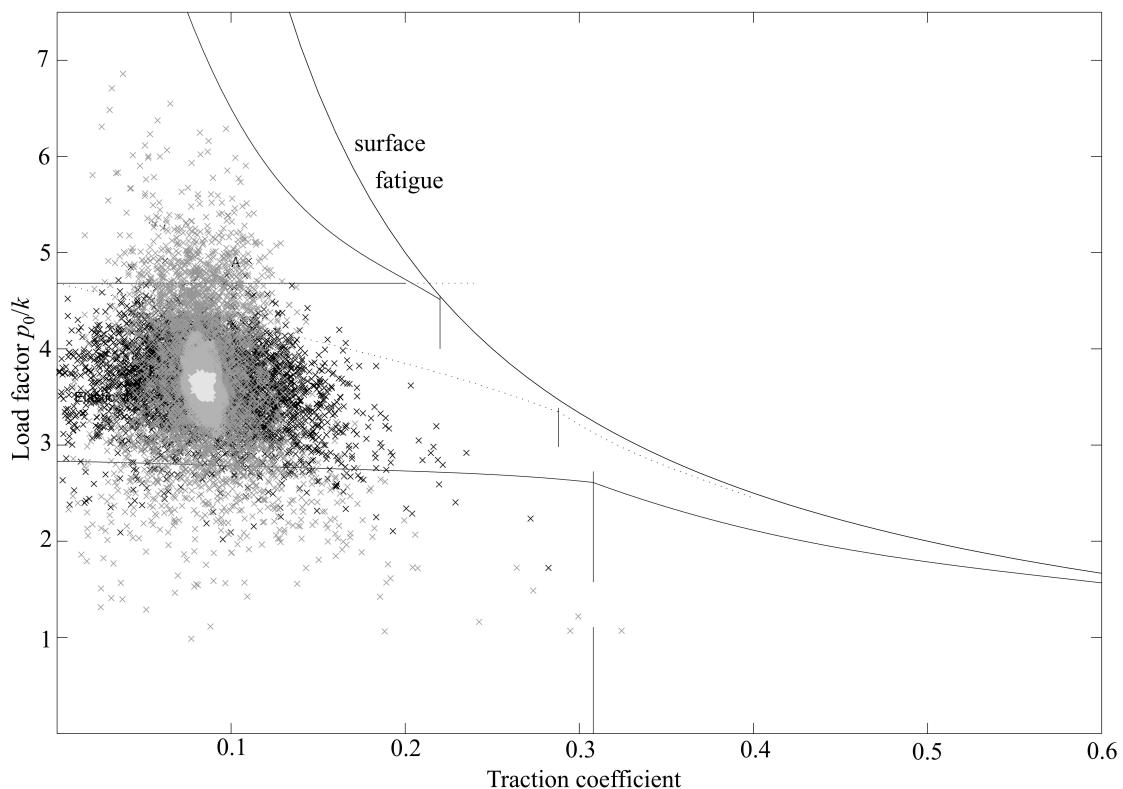


Figure 5 Shakedown diagram with limiting line of surface fatigue indicated. Combinations of normalized vertical loads and traction coefficients for an operational case are shown. Responses are evaluated using low-pass filter with cut-off frequency at 90 Hz (light grey), 200 Hz (grey) or 1000 Hz (dark grey) are compared to the non-filtered response (black). From [3].

Further analyses of the influence of corrugation and admissible levels under different types of operational conditions are planned by Chalmers.

4.3 Growth of large rail cracks

The studies on the influence of corrugation and out-of-round wheels discussed in sections 4.1 and 4.2 focused on the initiation and growth of small RCF cracks. This early stages are governed by the contact stress field and the simulations were carried out using an assumption of semi-infinite contact geometries.

In rails, as the crack grows the growth tends to be controlled by global bending and thermal stresses. The magnitude of the global bending is in turn influenced by the contact load magnitude. To investigate crack growth rates of larger rail cracks, a study was carried out. This study focused on the influence of rail temperature, and of high loads caused by the impact of flatted wheels. A major conclusion from the study was that large wheel flats are not of major concern regarding the growth of fatigue cracks. In contrast they are of major concern regarding the final fracture. The background and details of this finding are compiled in the paper in Appendix III.

In a continuation, numerical simulations are currently on the way to establish safety limits for cracks in rails. In these studies it has been shown that the bending moment in a rail is not only related to the magnitude of the impact force, but also to the frequency content of the impact force. A “worst-case scenario” of an impacting wheel flat has been established. This load is then employed to predict bending moments under different operational conditions. Stress intensity factors for different types of rail cracks subjected to bending and temperature loading are then derived and compared to the material’s fracture toughness. These studies are underway and will be included in a later Deliverable.

4.4 Influence of insulated joints

As mentioned in section 4.1, simulations of dynamic train–track interaction using FIERCE have been combined with RCF predictions using FIERCE and elasto-plastic finite element simulations to evaluate the influence of insulated rail joints on increases in dynamic loads and subsequent material deterioration. Details are given in the paper in Appendix IV.

In a subsequent study additional elasto-plastic simulations have been carried out. These focus on the plastic deformation at the insulated joint. The first results of these simulations quantify the increased plastic deformation and resulting fatigue impact if the insulation gap is made wider. Details are presented in Appendix V.

The work in WP4.2 on insulated joints is related to work in other work packages, such as WP4.5 (regarding maintenance aspects), SP1 and WP4.1 (statistics on operational failures) and SP5 (logistics of insulated joint solutions).

5. Numerical simulations of squats

TU Delft has carried out investigations on squats. These investigations concerned correlation analyses and numerical simulations of stresses, strains and fatigue in rails.

The correlation analysis was performed. It is concluded that squat occurrence can be related to track short wave irregularities, especially on the rail top such as indentations, weld and corrugations. Material strength, un-sprung mass, traction and braking, sleeper spacing and fastening system properties also play important roles.

The analysis of contact forces stresses, strains and fatigue featured a transient finite element model. Contact forces, stresses and strains are evaluated and a squat development process has been postulated.

Details are included in the papers in Appendices VI, VII and VIII.

5.1 Correlation analyses

To facilitate the numerical analyses, a correlation analysis was performed based on field inspections and on examining 122km of rails.

Apart from the clear relation with rail surface defects, correlation has been identified with track short wave irregularities. It suggests that the stiffness and damping characteristics of the track, particularly those of the rail and the rail pad, may have played a role.

It is also found that short-pitch/corrugation-like wave pattern of various severities can be seen in the neighbourhood of about 72% of the squats. This may suggest certain relationship between squats and corrugation: corrugation and squats may have occurred due to the same stiffness and damping properties of the track, though they may have developed independently; or the rail surface irregularities at some corrugation have caused large wheel-rail forces, therefore caused the squats around the corrugation; or it is a consequence of the two mechanisms combined: track local eigen characteristics cause both corrugation and squats to develop, and rail surface irregularities at corrugation speed up the development of squats.

5.2 Numerical models

A hybrid transient multi-body-Finite-Element (MB-FE) approach has been taken, see figure 5 for the model. Details are given in appendix V. The advantages are:

- The rail and the wheel are modelled with three-dimension FE mesh in the area of interest, detailed stresses and strains in the contact area and in the bulk materials can be studied.
- The parts farther away can be modelled with coarse mesh or with rigid body, where appropriate, so that the effects of the vehicle and the track can all be simultaneously taken into account, with affordable computing costs.
- The short wave/high-frequency dynamics characteristics of the problem can therefore be fully taken into account in the calculation of the stress and strain states. Wave propagation in the continua is also accounted for.
- Friction is considered in the contact. Therefore not only the dynamic vertical force, but also the dynamic tangential force is fully accounted for.
- Non-linear material properties, such as plasticity, can be taken into account. Material behaviour under high hydrostatic pressure can also be modelled.
- Arbitrary contact geometry can be modelled.

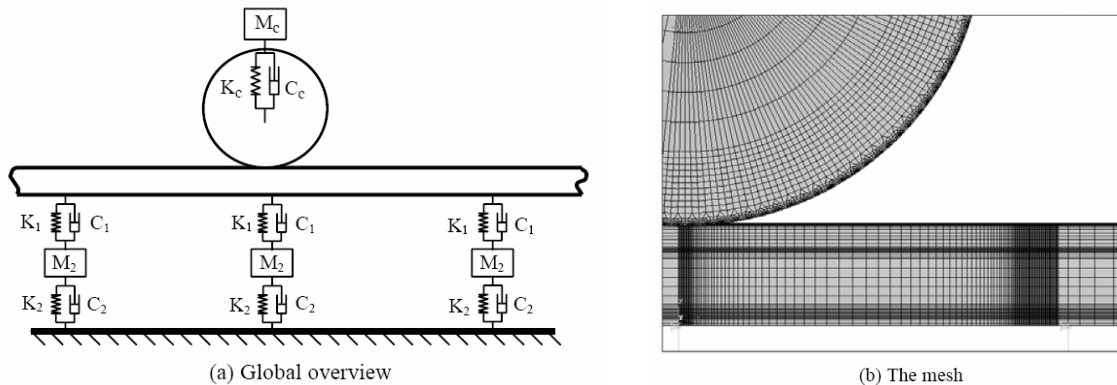


Figure 5 The hybrid MB-FE model

The model has been validated in the following aspects:

- Calculated wavelength of contact force is in agreement with that of the wave pattern following squats, observed in the field. See appendix V.
- Results in contact force, stress and strain levels, and their positions show good correspondence with field observations. See appendix V.
- Calculated residual stress is in agreement with measurement See appendix VI.
- Contact area and pressure are validated against Hertz results in the quasi-static state. See appendix VII.

5.3 Influence of rail top irregularities and material strength

The influence of geometrical irregularities and material strength has been investigated. Details are presented in appendices V and VI. Further analyses will be carried out based on more measured geometry. Attempt will also be made to investigate the effect of material strength under high hydrostatic pressure.

It should be noted that the difference in the shapes of contact forces in appendices V and VI is due to the difference in the model structure, one representing the case which may cause squats to initiate (appendix V), and the other may not (appendix VI). Systematic discussion of that will be presented in later publications.

5.4 Influence of traction/braking and unsprung mass

It is observed in the correlation analysis that more squats are found near stations and signals where traction and braking efforts are high. Numerical analysis shows that friction level, hence tangential force plays an important role in the magnitude of plastic strain. Details are presented in appendix V.

The effect of unsprung mass of vehicle is also investigated. It is found that in the high frequency domain, the unsprung mass on the axle does not result in an extra dynamic load to the first peak force due to lag in wave propagation. On the other hand unsprung mass close to the contact area, such as the mass of the tyre, can lead to an extra dynamic force which can be 12 times that of the additional mass. Details are given in appendix VI.

5.5 Influence of welds of continuously welded rails

Welds, both thermite and flash butt, are vulnerable to squats. Out of a field survey of 65 squats, 11 are found at welds, that is 17% of the total. The high percentage of squats at welds may be explained by two main factors: material strength/hardness and longitudinal rail top profile. Analyses of the effects of strength and

geometry deviation have been carried out, and the inadequacy of existing standard for weld finish geometry is discussed in appendices V and VI.

Weld material strength data have been obtained from Corus for further investigation.

5.6 A squats growth process is postulated

A squat development process has been postulated based on the correspondence between on the one side the calculated contact force magnitude and its wavelength and on the other side the field-observed squat dimension and the wave pattern following them. The wave length is between 20 – 40 mm. When the traffic speed is about 140km/h, which is typical on the Dutch railway, the frequency is about 1000 – 2000 Hz. It bears resemblance to short wave corrugation.

The postulated squats growth process is as follows:

- (1) **For a class A squat growing into class B:** As is shown in figure 6, with proper size, position, track and traffic conditions,
 - a. A typical squat A will has a first impact with a passing wheel at B_1 of (b) (i.e. B_{1G} of (a)), causing a peak contact force B_1 of (c). This peak force after many wheel passages turns point B_1 of (b) into B_2 of (d).
 - b. Then a second peak force C_1 of (c) follows. This peak force first causes the wave C_1 of (b) in the early stage of the squat-A-growing-into-B process, and then gradually turns wave C_1 into the large plastic deformation between B_2 and C_2 . This is to say that in such a process the part of rail top surface between B_1 and C_1 deforms gradually into part of the squat (the part between B_2 and C_2). This is in agreement with many field observations, as is shown in figures 1 and 2.
 - c. In the process of turning wave pattern C_1 into part of the squat, there may be for certain period no wave pattern after (i.e. to the right of) C_1 and C_2 , because the force peak D_1 is not yet large enough to make a new visible wave pattern.

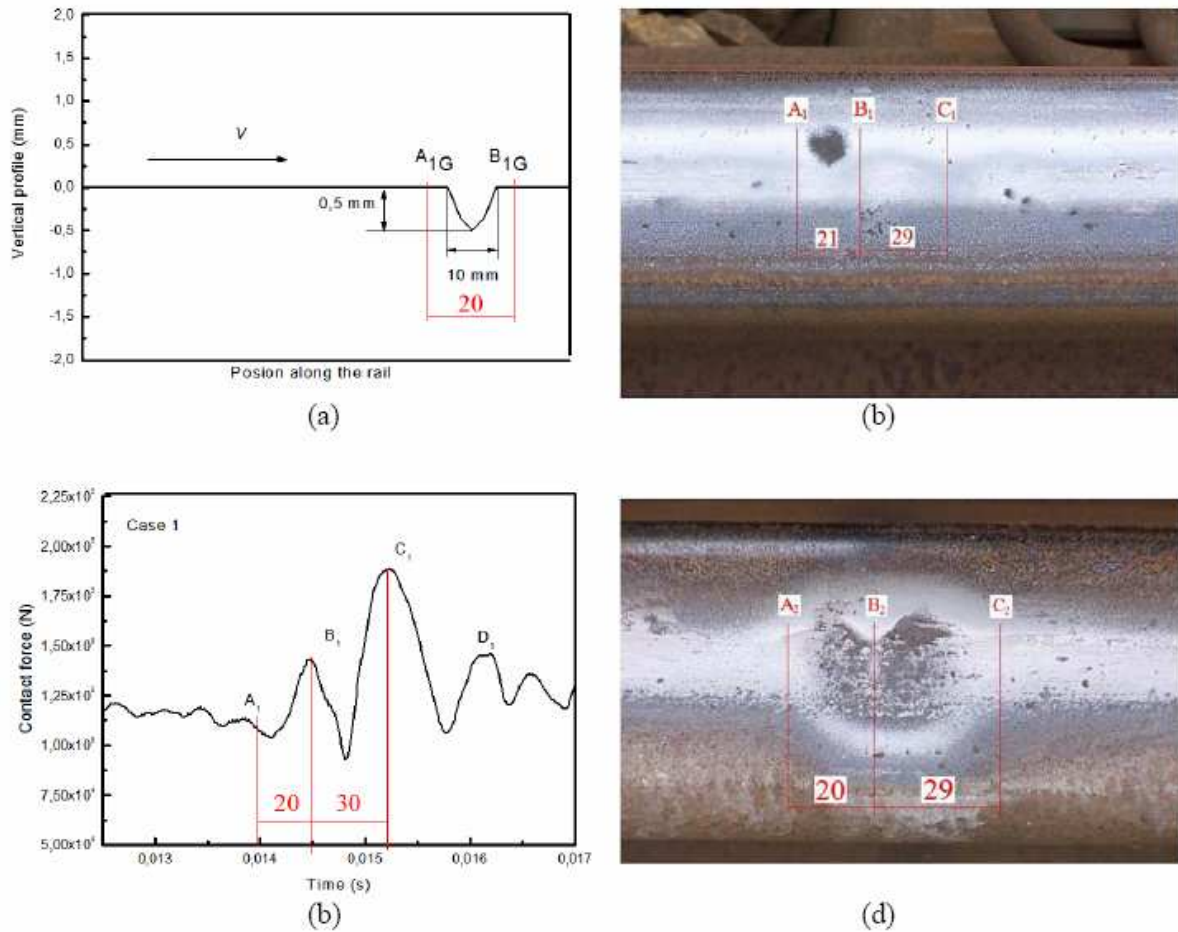


Figure 6 How a class A squat grow into class B

Traffic travels from left to right.

- (a) Geometry of typical squats A used for the FE model, one of such is shown in (b);
- (b) A typical squat A with typical wave pattern after it due to dynamic contact force shown in (c);
- (c) The calculated contact force caused by the geometry of (a). Notice that peak B₁ is a forced vibration, while peaks C₁ and D₁ are free vibration
- (d) A typical squat B

The red numbers indicate the distances (mm) between the A, B and C points. Subscripts 1 and 2 designate the 2 squat geometries simulated in figures 6 and 7. Subscript G indicates that it is the points on the simulated geometry. Note that the squats in (b) and (d) are two different squats.

Notice the similarity between the wave patterns of (b) and (c), it is postulated that A₁ of (b) is A₂ of (d), while B₁ becomes B₂ and C₁ becomes C₂.

- (2) **For a class B squat growing into class C:** As is shown in figure 7,
 - a. The squat B, together with other track and traffic conditions, causes large impact force so that the squat grows into class C. Wave patterns such as D₂ develop after C₂.
 - b. When a squat C develops further, the wave patterns marked with A₂, B₂, C₂ and D₂ may be wiped out by the large impact force.

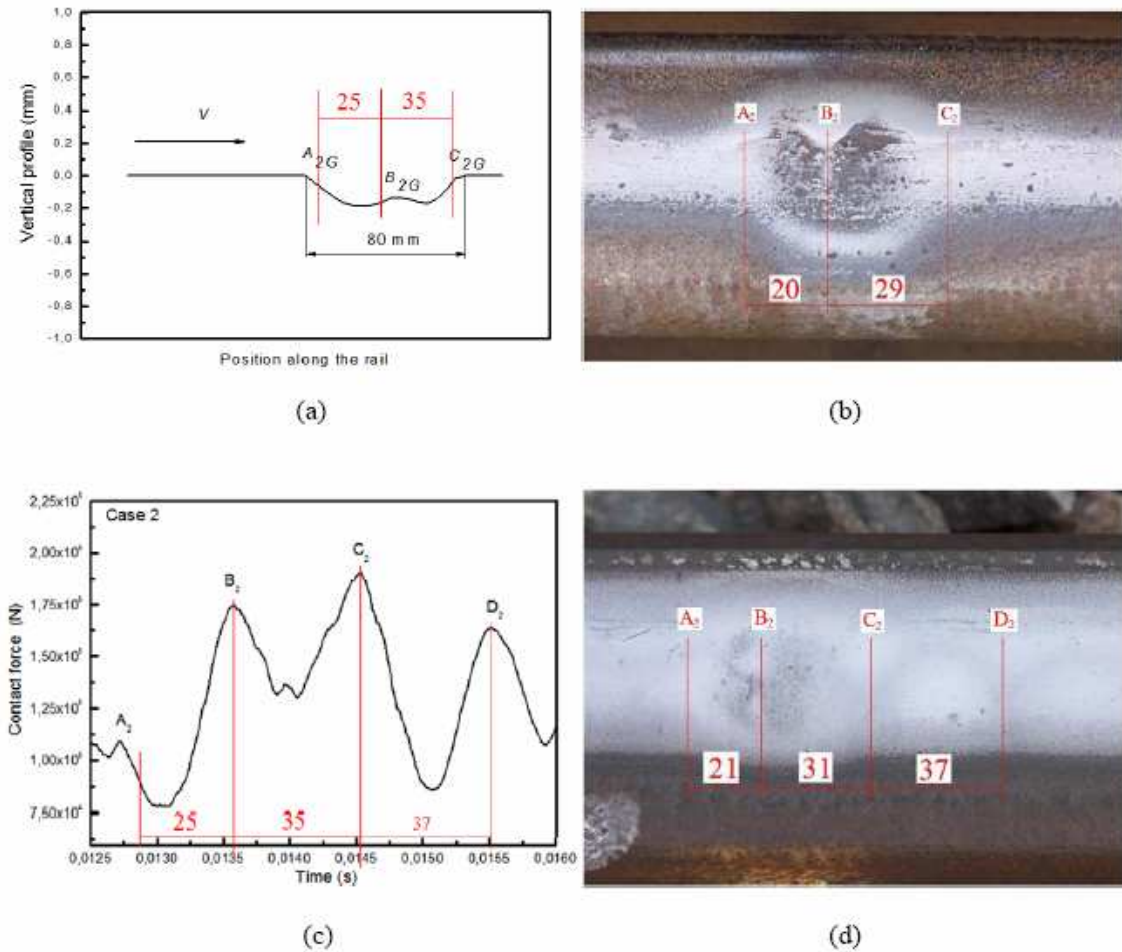


Figure 7 How a class B squat grow into class C

Traffic travels from left to right.

- (a) Geometry of typical squats B and C used for the simulation, as are shown in (b) and (d);
- (b) A typical squat B (it is the same as (d) of figure 6);
- (c) The contact force caused by the geometry of (a). Notice that the wavelength between A_2 , B_2 and C_2 of (c) follows the geometry of (a), as it should be in a forced vibration, while the wavelength C_2 - D_2 of (c) does not because it is free vibration;
- (d) A typical squat C with typical wave pattern after it due to dynamic contact force shown in (c);

Convention is the same as figure 6. Note that the squats in (b) and (d) are two different squats.

Notice the similarity between the wave patterns of (b), (c) and (d). Compared with (b), (d) has now a new wave D_2 after C_2 , caused by the larger peak force D_2 .

The small discrepancies between the wavelengths of (a) – (d), e.g. the different distances between A_2 - B_2 , may be explained by the fact that the larger the squat deformation, the larger the dynamic contact force, and therefore the larger wavelength. The fundamental mechanism behind it is the excitation of more lower frequency components.

The monitoring conducted by ProRail and TU Delft will provide data for the validation of this postulation.

References

- [1] Li, Z., Zhao, X., Esveld, C. and Dollevoet, R., *Causes of Squats: Correlation Analysis and Numerical Modeling*, Proc. of the 7th International Conference on Contact Mechanics and Wear of Rail/Wheel Systems (CM2006), September 24-27, 2006, Brisbane, Australia, 439-446

- [2] Li, Z. Zhao, X. Esveld, C. and Dollevoet, R., *Rail Stresses, Strain and Fatigue under Dynamic Wheel-Rail Interaction*. Accepted for 2007 IHHA Specialist Technical Session, June 11 – 13, 2007 at Kiruna, Sweden
- [3] Zhao, X., Li, Z., Esveld, C. and Dollevoet, R., *The Dynamic Stress State of the Wheel-Rail Contact*, Proc of the 2nd IASME/WSEAS International Conference on Continuum Mechanics, 15-17 May, 2007, Portoroz, Slovenia, 127-133

6. The effect of material characteristics on material deterioration

University of Newcastle has compiled a state-of-the-art regarding the influence of material characteristics on the material deterioration.

The report sets out with an overview of key micro-structural and material properties, which are used to grade and classify different rail steels. This is followed by a review of main wear and cracking mechanism, and an indication on how wear and crack growth can interact to determine rail life. In particular the whole life rail model and the influence of wear truncation are described.

Details are found in the state-of-the-art report in Appendix IX.

The relation to practical rail management issues are discussed in the paper in Appendix X.

7. Conclusions

In this tentative report we present a description of the work carried out within approximately the first nine months regarding the influence of rail/joint degradation on operational loads and subsequent deterioration. From the different partners the input includes

- Banverket** Measurements of axle loads on selected lines that are aimed at providing input to simulations of dynamic train–track interaction
- Prorail/TU Delft** Descriptions of on-going and planned in-field monitoring of squats. These aim at providing possibilities to validate numerical predictions. Numerical simulations of train–track interaction and deterioration in the presence of rail squats. The results are to be used in preventing squats and defining maintenance procedures. An analysis of correlation between the occurrence of squats and pertinent operational parameters. These are vital in identifying possibilities for improvements. In-depth analysis of the dynamic state of stress in the wheel–rail contact.
- voestalpine** A catalogue of material characteristics of rail steels. These material data provide input to numerical simulations of rail degradation.
- Univ Newcastle** A state-of-the-art report on the effect of material characteristics on material deterioration with particular focus on the interaction with numerical modelling, in particular featuring the whole-life rail model and with emphasis on wear truncation. A study on the practical application of theoretical knowledge in managing the wheel–rail interface.
- Chalmers** A numerical study of the influence of corrugation on contact load magnitudes and pertinent rolling contact fatigue impact. The results are of use in defining allowable corrugation magnitudes. A numerical study of the influence of wheel flats on contact load magnitudes, and pertinent crack growth and risk of fracture. The results and derived models provide a basis for defining allowable crack sizes under different operational conditions. A preliminary numerical study of plastic deformations and fatigue of the rail material at insulated joints. The results are a first step in the optimization of insulated joints.

The output of the deliverable is highly linked to the establishment of minimum action rules in that the work in this Deliverable provides a basis for the numerical tools needed to specify minimum action rules.

8. Annexes

It should be noted that some appendices relates to work that has been carried out (partly or in whole) before the start of the INNOTRACK project. These are included since they are deemed essential in providing a more coherent image of the context of the work that has and will be carried out within INNOTRACK.

- I. voestalpine, **Rail steel grade data**, 27 pp.
- II. Anders Ekberg, Elena Kabo, Jens Nielsen & Roger Lundén, **Subsurface initiated rolling contact fatigue of railway wheels as generated by rail corrugation**, *accepted for publication in International Journal of Solids & Structures*, 25 pp.
- III. Johan Sandström & Anders Ekberg, **Predicting crack growth and risks of rail breaks due to wheel flat impacts in heavy haul operations**, *Proceedings of IHHA – International Heavy Haul Conference*, June 11–13, 2007, Kiruna, Sweden, 10 pp. (w. minor revision)
- IV. Elena Kabo, Jens Nielsen and Anders Ekberg, **Prediction of dynamic train/track interaction and subsequent material deterioration in the presence of insulated rail joints**, *Vehicle System Dynamics*, vol 44, Supplement, 2006, pp 718–729. (preprint version)
- V. Johan Sandström, Anders Ekberg & Elena Kabo, **Insulated joints – comparison between 4 mm and 8 mm joint gap**, 6 pp.
- VI. Zili Li, Xin Zhao, Coenraad Esveld & Rolf Dollevoet, **Causes to squats: correlation analysis and monitoring**, *Proceedings 7th International Conference on Contact Mechanics and Wear of Rail/Wheel Systems*, 24th – 27th September 2006, Brisbane, Australia, 8 pp.
- VII. Zili Li, Xin Zhao, Coenraad Esveld & Rolf Dollevoet, **Rail stresses, strains and fatigue under dynamic wheel–rail interaction**, *Proceedings of IHHA – International Heavy Haul Conference*, June 11–13, 2007, Kiruna, Sweden, 7 pp.
- VIII. Xin Zhao, Zili Li, Coenrad Esveld, Rolf Dollevoet, **The dynamic stress state of the wheel–rail contact**, *Proceedings of 2nd IASME/WSEAS International Conference on Continuum Mechanics*, May 15-17, 2007, Portoroz, Slovenia, pp 127–133.
- IX. DI Fletcher, FJ Franklin, A Kapoor, **State-of-the-art report on the effect of material characteristics on material deterioration**, 25 pp.
- X. Ajay Kapoor, Felix Schmid and David Fletcher, **Managing the critical wheel/rail interface**, *Railway Gazette International*, January 2002, pp 25–28. (w. minor revision)